Electronic Supplementary Information

Origin of unique hyper-Raman signals of trifluoroethanol

Kai-Chin Chien[a], Surajit Maity[a], and Hirotsugu Hiramatsu [*a]

a. Department of Applied Chemistry and Institute of Molecular Science, National Yang Ming Chiao Tung University, Hsinchu, 30010, Taiwan

1. Consideration of laser power

In our experiments, the HR process is excited using a 15 ps-pulsed laser at 532 nm, delivering a typical output of 200 mW with a repetition of 200 kHz (1 μJ/pulse). The peak power reaches 66.7 kW. When the Gaussian laser beam (wavelength λ) having the diameter w_0 is focused with a lens having the focal length f, the laser spot size w is calculated as

$$w = \frac{M^2 \lambda f}{\pi w_0}.$$

Considering the parameters [λ = 532nm, w_0 = 1.4mm, M^2 = 1.0 (ideal case for simplicity), and f = 15 mm], w is calculated to be 1.81 μm (1.81e-4 cm). Therefore, the estimated power density at the focal point is 66.7kW / πw^2 = 6.4 × 10^{11} W/cm^2.

This value is comparable to the power density in an examination of the multiphoton ionization of H_2O, where the power density is set to 10^{11} – 10^{12} W/cm^2 at 3-5 eV [2] and the plasma formation with 532 nm laser at ~10^{11} W/cm^2.[3] Even though the phenomena studied in these papers differ from our case, our condition is considered to be sufficient to induce the non-linear optical processes of water such as the radical formation due to the three-photon excitation.

2. Hyper-Raman spectrum of sodium ethoxide ($CH_3CH_2O^-$ Na^+)

21% sodium ethoxide in ethanol solution was purchased from Thermofisher Scientific. The HR spectrum was recorded without further purification. We detected the HR bands of ethanol as the solvent. A few additional bands are assignable to ethoxide anion. The peak position and intensity were different from those of the unique HR bands in Fig. 1a.

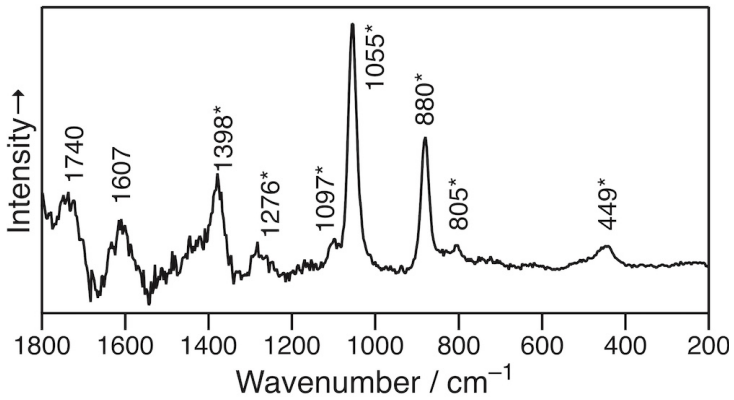

Figure S1 HR spectrum of 21% sodium ethoxide in ethanol (asterisk indicates the solvent bands).

3. Fluorescence spectrum of telephthalic acid as a probe molecule of the hydroxyl radical

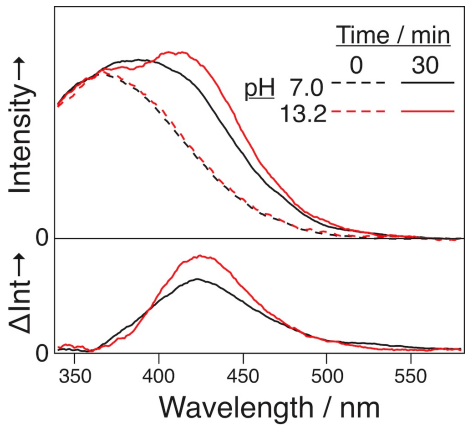

Figure S2 Fluorescence spectrum of 1 mM telephthalic acid in aqueous solution at pH 7.0 (black) and 13.2 (red) before (chain lines) and after (solid lines) the irradiation of the 532 nm ps-pulse laser for 30 min. The difference (solution minus solvent) spectra are shown in the lower panel. Excitation wavelength in fluorescence spectroscopy is 310 nm. The difference spectrum shows a peak at 426 nm. This fluorescence peak is due to the formation of hydroxyterephthalate, which is formed via the reaction of TA and the hydroxyl radical (OH•). The emergence of the peak at around 425 nm indicates the presence of OH• in the solution.[1]

4. Effects of additive compounds on hyper-Raman spectrum of TFE in aqueous solution

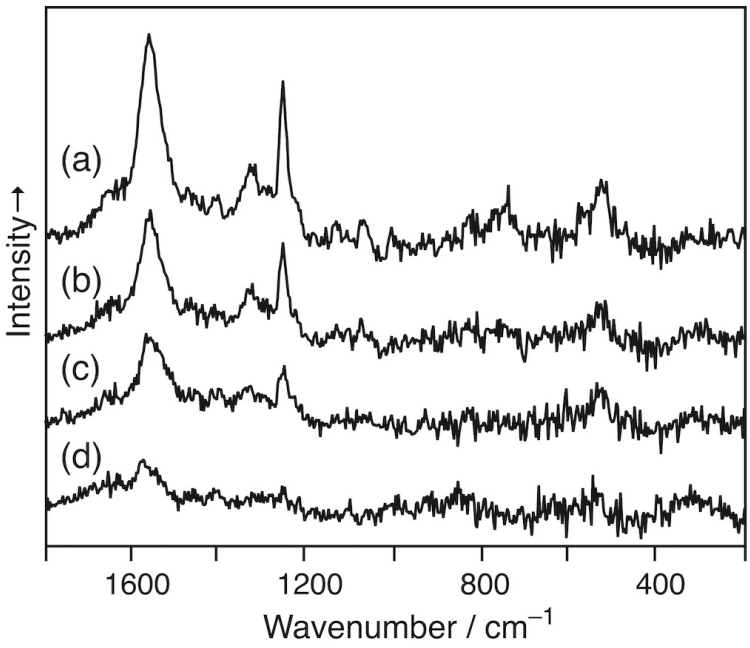

Figure S3 HR spectrum of 50 mM TFE aqueous solution at pH 13.2 (a), and with (b) O_2 bubbling, (c) 50 mM *n*-butanol, (d) 10 mM H_2O_2.

5. Derivation of the TFE concentration dependence of products and intermediates based on steady-state approximation

By analogy to the case of MeOH,[4] we considered the following reactions of TFE and the hydroxyl radical ($OH^{\bullet}$). At the neutral pH, the reaction is;

$H_2O \rightarrow H^{\bullet} + OH^{\bullet}$	(1): photodissociative formation of $H^{\bullet}$ and $OH^{\bullet}$
$CF_3CH_2OH + OH^{\bullet} \rightarrow CF_3C^{\bullet}HOH + H_2O$	(2): formation of TFE radical
$2CF_3C^{\bullet}HOH \rightarrow (CF_3CHOH)_2$	(3a):dimerization of TFE radical
$2CF_3C^{\bullet}HOH \rightarrow CF_3CH_2OH + CF_3CHO$	(3b):disproportionation of TFE radical
$CF_3CH^{\bullet}OH + O_2 \rightarrow CF_3CH(OH)OO^{\bullet}$	(4): peroxidation of TFE radical

[The rate constant of each step was set to k_1, k_2, k_{3a}, k_{3b}, and k_4, respectively.]

According to the steady-state approximation, we can assume that

$$\frac{d[\mathrm{TFE}^{\bullet}]}{dt} = k_2[\mathrm{TFE}][\mathrm{OH}^{\bullet}] - k_{3a}[\mathrm{TFE}^{\bullet}]^2 - k_{3b}[\mathrm{TFE}^{\bullet}]^2 = 0$$

It leads that

$$[\mathrm{TFE}^{\bullet}] = \sqrt{\frac{k_2}{k_{3a}+k_{3b}}[\mathrm{TFE}][\mathrm{OH}^{\bullet}]} \qquad (5')$$

$$[\mathrm{TFE}_2] = k_{3a}[\mathrm{TFE}^{\bullet}]^2 = \frac{k_2 k_{3a}}{k_{3a}+k_{3b}}[\mathrm{TFE}][\mathrm{OH}^{\bullet}] \qquad (6')$$

The reaction proceeds under the basic condition (pH 13.2). The OH group should be mostly deprotonated. Therefore, each species should exist in the equilibrium between the neutral and anionic forms.

6. Procedure of singular value decomposition analysis and reconstruction

The two-dimensional (2D) matrix data M that consists of the spectral data at each concentration was analyzed by a method based on singular value decomposition (SVD).[5,6] In this analysis, m (= 5) spectra having n (= 520) points in M is decomposed into a product of matrices U = ($\boldsymbol{u}_1$ $\boldsymbol{u}_2$ … $\boldsymbol{u}_n$) (concentration dependence), W (singular values), and V = ($\boldsymbol{v}_1$ $\boldsymbol{v}_2$ … $\boldsymbol{v}_n$) (spectral components):

$$\mathrm{M} = \mathrm{UWV}^{\mathrm{T}} \qquad (1)$$

and $\boldsymbol{u}$ and $\boldsymbol{v}$ are the $m \times 1$ and $n \times 1$ vectors, respectively. W is the diagonal matrix in which w_{ii} shows the singular value of the i-th components (Figure 3a, inset). We disregard the three components corresponding to the small w_{jj} ($j > l$) and confine our attention to the limited number of components by reserving a reduced $l \times l$ dimensional matrix W_l (note that l = 2 for this time) and the corresponding components in U and V, i.e.,

$$\begin{aligned} \mathrm{M} &= \mathrm{U}_l\mathrm{W}_l{\mathrm{V}_l}^{\mathrm{T}} + \mathrm{N} \\ &\approx \mathrm{U}_l\mathrm{W}_l{\mathrm{V}_l}^{\mathrm{T}} \end{aligned} \qquad (2)$$

where U_l is ($\boldsymbol{u}_{\mathrm{r}1}$ $\boldsymbol{u}_{\mathrm{r}2}$ … $\boldsymbol{u}_{\mathrm{r}l}$), V_l is ($\boldsymbol{v}_{\mathrm{r}1}$ $\boldsymbol{v}_{\mathrm{r}2}$ … $\boldsymbol{v}_{\mathrm{r}l}$), and N is the residual. We can place an $l \times l$ matrix K (and K^{-1}) to reconstruct M to be the product of U_l' and V_l':

$$\mathrm{U}_l\mathrm{W}_l{\mathrm{V}_l}^{\mathrm{T}} = (\mathrm{U}_l\mathrm{K})(\mathrm{K}^{-1}\mathrm{W}_l{\mathrm{V}_l}^{\mathrm{T}}) = \mathrm{U}_l'{\mathrm{V}_l'}^{\mathrm{T}}, \qquad (3)$$

where U_l' [= ($\boldsymbol{u}_{\mathrm{r}1}$ $\boldsymbol{u}_{\mathrm{r}2}$ … $\boldsymbol{u}_{\mathrm{r}l}$)] and V_l' [= ($\boldsymbol{v}_{\mathrm{r}1}$ $\boldsymbol{v}_{\mathrm{r}2}$ … $\boldsymbol{v}_{\mathrm{r}l}$)] are the reconstructed matrices. The ij-th element k_{ij} of K is set such that $\boldsymbol{u}_{\mathrm{r}i}$ is consistent with f_i(t) as the model function of the concentration dependence of the i-th species. As a result, $\boldsymbol{v}_{\mathrm{r}l}$ is derived.

7. Calculated results of radical anions of TFE and TFE_2

Vibrational frequencies of the radical anions of TFE and TFE_2 were calculated at CAM-B3LYP/aug-cc-pVDZ using Gaussian 16. Two H_2O molecules were allocated near each oxygen atom of TFE to take account of the effect of the hydrogen bonding in an aqueous solution.

Table S1 lists the vibrational frequencies and their assignment. The vibrational motion of each mode is illustrated in Figure S4.

Table S1 Vibrational frequencies of radical anions of TFE and TFE_2 calculated at CAM-B3LYP/aug-cc-pVDZ

Peak position / cm^{-1}		
$TFE^{\bullet-}$	d_2-$TFE^{\bullet-}$	Assignment
1546.3423	1531.4283	ν(C-O)
1319.2559		δ(C-H)
1233.4174	1230.3207	ν(C-C)
1097.2629	1106.2302	δ(C-C-O)
	1005.1821	δ(C-D)
$TFE_2^{\bullet-}$	$(d_2\text{-}TFE)_2^{\bullet-}$	
1561.392	1515.4245	ν(C-O), in-phase
1487.9317	1431.974	ν(C-O), out-of-phase
1366.4455		δ(C-H), in-phase
1349.4816		δ(C-H), out-of-phase
1298.1795	1291.5366	ν(C-C), in-phase
1265.2272	1279.0206	ν(C-C), out-of-phase
	1199.9471	δ(C-C-D)§
	1195.3131	δ(C-C-D)§
1178.4094		δ(C-F) +δ(C-H)
1172.1077		δ(C-F) +δ(C-H)
1123.2711	1120.9804	ω(C-C-O)§
1105.9443	1104.6443	ω(C-C-O)§
	1022.4107	δ(C-D), in-phase
	994.31	δ(C-D), out-of-phase

§ localized vibration at each subunit

With regard to the isotope effects upon the d_2 labeling, we found remarkable effects in (i) lower peak shift of the largest band from 1558 to 1518 cm^{-1} and (ii) fading of the bands at 1257 and 1329 cm^{-1} (Figure 1). The calculation suggests that (i) the C-O stretching band of $TFE^{\bullet-}$ (Figures S5a) shifts lower from 1546.3 to 1531.4 cm^{-1} and those of $TFE_2^{\bullet-}$ (Figures S5b) from (1561.4 and 1487.9 cm^{-1}) to (1515.4 and 1432.0 cm^{-1}). Also, the CH

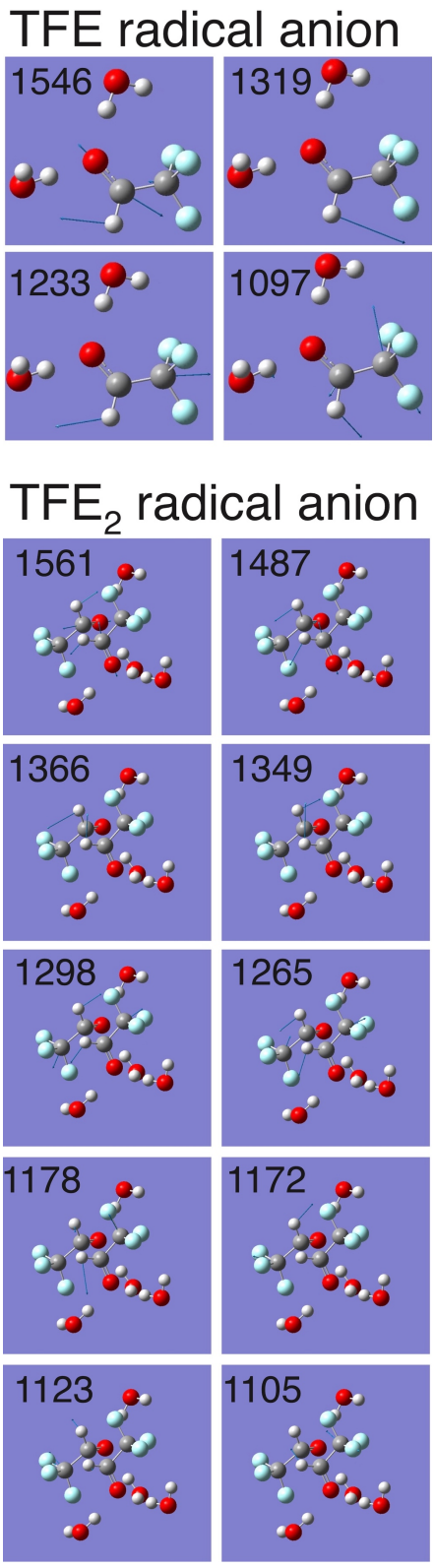

Figure S4 Displacement vector of each atom with molecular vibrations.

bending band of $TFE^{\bullet-}$ shifts from 1319.3 cm^{-1} to 1005.2 cm^{-1} and those of $TFE_2^{\bullet-}$ shifts lower from (1349.5 and 1366.4 cm^{-1}) to (994.3 and 1022.4 cm^{-1}). Even though the calculation does not completely reproduce the observed frequencies of the HR bands, it explains the lower peak shift of the HR bands due to the d_2 labeling.

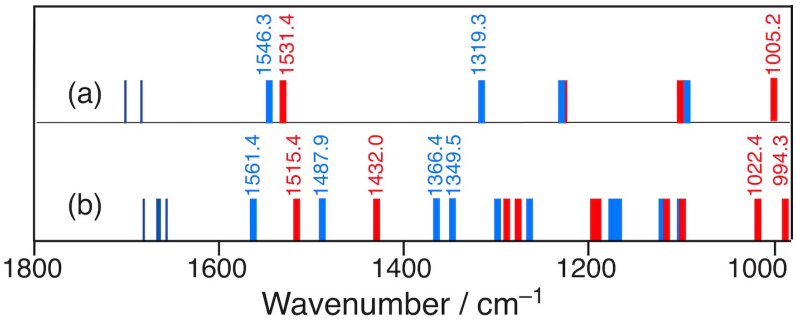

Figure S5 Calculated vibrational frequencies of $TFE^{\bullet-}$ (a) and $TFE_2^{\bullet-}$ (b). Thin lines above 1600 cm^{-1} indicates the vibrations of added H_2O.

References

1. T. J. Maton, J. P. Lorimer, D. M. Bates and Y. Zhao, *Ultrason. Sonochem.*, 1994, **1**, S91-S95.
2. R. A. Crowell and D. M. Bartels, *J. Phys. Chem.*, 1996, **100**, 17940-17949.
3. A. Vogel, K. Nahen, D. Theisen and J. Noack, *IEEE J. Sel. Top Quantum Electron*, 1996, **2**, 847-860.
4. G. Heit, A. Neuner, P.-Y. Saugy and A. M. Braun, *J. Phys. Chem. A*, 1998, **102**, 5551-5561.
5. J. Jaumot, M. Vives and R. Gargallo, *Anal. Biochem.*, 2004, **327**, 1-13.
6. N. Kumar, A. Bansal, G. S. Sarma and R. K. Rawal, *Talanta*, 2014, **123**, 186-199.